Core-hole effects in the x-ray-absorption spectra of transition-metal silicides

P. J. W. Weijs, M. T. Czyżyk, and J. F. van Acker
Research Institute for Materials, Faculty of Science, University of Nijmegen, Toernooiveld, NL-6525 ED Nijmegen, The Netherlands

W. Speier*
Institut für Festkörperphysik der Kernforschungsanlage Jülich, D-5170 Jülich 1, Federal Republic of Germany

J. B. Goedkoop, H. van Leuken,† H. J. M. Hendrix, and R. A. de Groot
Research Institute for Materials, Faculty of Science, University of Nijmegen, Toernooiveld, NL-6525 ED Nijmegen, The Netherlands

G. van der Laan‡
Materials Science Center, Groningen University, Nijenborg 18, NL-9747 AG Groningen, The Netherlands

K. H. J. Buschow
Philips Natuurkundig Laboratorium, Postbus 80 000, NL-5600 JA Eindhoven, The Netherlands

G. Wiech
Sektion Physik, Ludwig-Maximilians-Universität München, D-8000 München 22, Federal Republic of Germany

J. C. Fuggle
Research Institute for Materials, Faculty of Science, University of Nijmegen, Toernooiveld, NL-6525 ED Nijmegen, The Netherlands

(Received 26 January 1990)

We report systematic differences between the shape of the Si K x-ray-absorption spectra of transition-metal silicides and broadened partial densities of Si p states. We use a variety of calculations to show that the origin of these discrepancies is the core-hole potential appropriate to the final state. The effects can be successfully described by *ab initio* supercell calculations which explicitly include the presence of the hole in the excited state. A Clogston-Wolff model, with the ground-state partial densities of states at the site to be ionized as input data, can also describe the core-hole effect and is found to be a useful tool for the understanding of core-hole effects.

I. INTRODUCTION

In x-ray absorption an electron is excited from a core level into a previously unoccupied electronic state above the Fermi level E_F. X-ray absorption is a local process obeying dipole selection rules, so that in the independent-electron model it would be directly related to the partial density of $l+1$ and $l-1$ states on the core ionized atom (l is the angular-momentum quantum number of the core state).[1] However, three effects make the relationship between partial density of states (DOS) and x-ray-absorption spectra (XAS) less direct. The first is the influence of the single-particle matrix elements, which must take into account the variation of the radial part of the final-state wave functions with final-state energy. The second effect is that of the effective potential of the core hole created. This is known to distort the local density of states around the core ionized site, and the effects may be very complex for narrow conduction bands with possibly large multiplet interactions.[2,3] The third class of effects includes the dynamical distortions of the spectrum due to the fact that the Hamiltonian controlling the "spectator" electrons in the initial and final states is not the same. This third class of effects leads to satellites and singularities in the spectra.[4–7] Strictly speaking, separation of the second and third effects enumerated here is not possible, but it is useful for a "zeroth-order" analysis and approximate description of the phenomena.

We note that an understanding of core-hole effects in general is necessary not only for XAS studies of unoccupied-state densities, but also for full understanding of phase shifts in structural studies using near-edge and extended x-ray-absorption fine structure (NEXAFS and EXAFS), to interpret the spectral function of many Auger transitions, and to analyze the dynamics and satellite structures in photoemission, x-ray emission, and other techniques involving creation or annihilation of core holes.[6,7] However, although this problem was recognized more than 30 years ago,[8] there is still little quantitative understanding of its relative importance. For instance, for Si, which is the element considered here, some authors have given evidence for core-hole effects in

Auger[9–11] and XAS,[12,13] while others have suggested no core-hole effect is present for XAS.[14]

In this paper we will discuss the Si K ($1s$) absorption spectra of transition-metal silicides and show that, in this case, the second of the effects listed above, the core-hole potential, is the most important influence on the spectral function once the solid-state electronic structure has been taken into account.

To put our work in context we take the unusual step of presenting our first results in the introduction. Figure 1 shows the Si K ($1s$) XAS spectra of a series of transition-metal silicides. The spectra all show a low intensity at threshold, followed by a series of peaks and shoulders before a long plateau region is observed. The spectral features must be related to structure in the unoccupied (mostly antibonding) states of Si p symmetry, because of the dipole selection rules and the local character of XAS. However, comparison with the calculated ground-state partial densities of states shown in Fig. 1 reveals a systematic difference: the experimental spectra consistently exhibit more weight near E_F than the calculations. When we observed these differences we hypothesized that they were due to core-hole effects.[12] In this paper we present evidence that this is indeed the case.

The paper is organized to first give experimental details in Sec. II A. Then, in Sec. II B we describe our band-structure calculations and in particular the supercell methods and the generalized Clogston-Wolff (CW) model used to to simulate the influence of a core hole. In this section we also describe the simulation of experimental and lifetime broadening. Section III A gives a description of the band-structure results and Sec. III C discusses their relation to experimental data. Here emphasis is also placed on comparison with another type of spectroscopy in which a core hole distorts the spectral function, the KLV Auger process. This comparison clearly establishes the validity of the computational methods. Section III D contains a discussion of simple model calculations to simulate the XAS and Auger spectra from ground-state DOS. Section III E gives comparison of the model calcu-

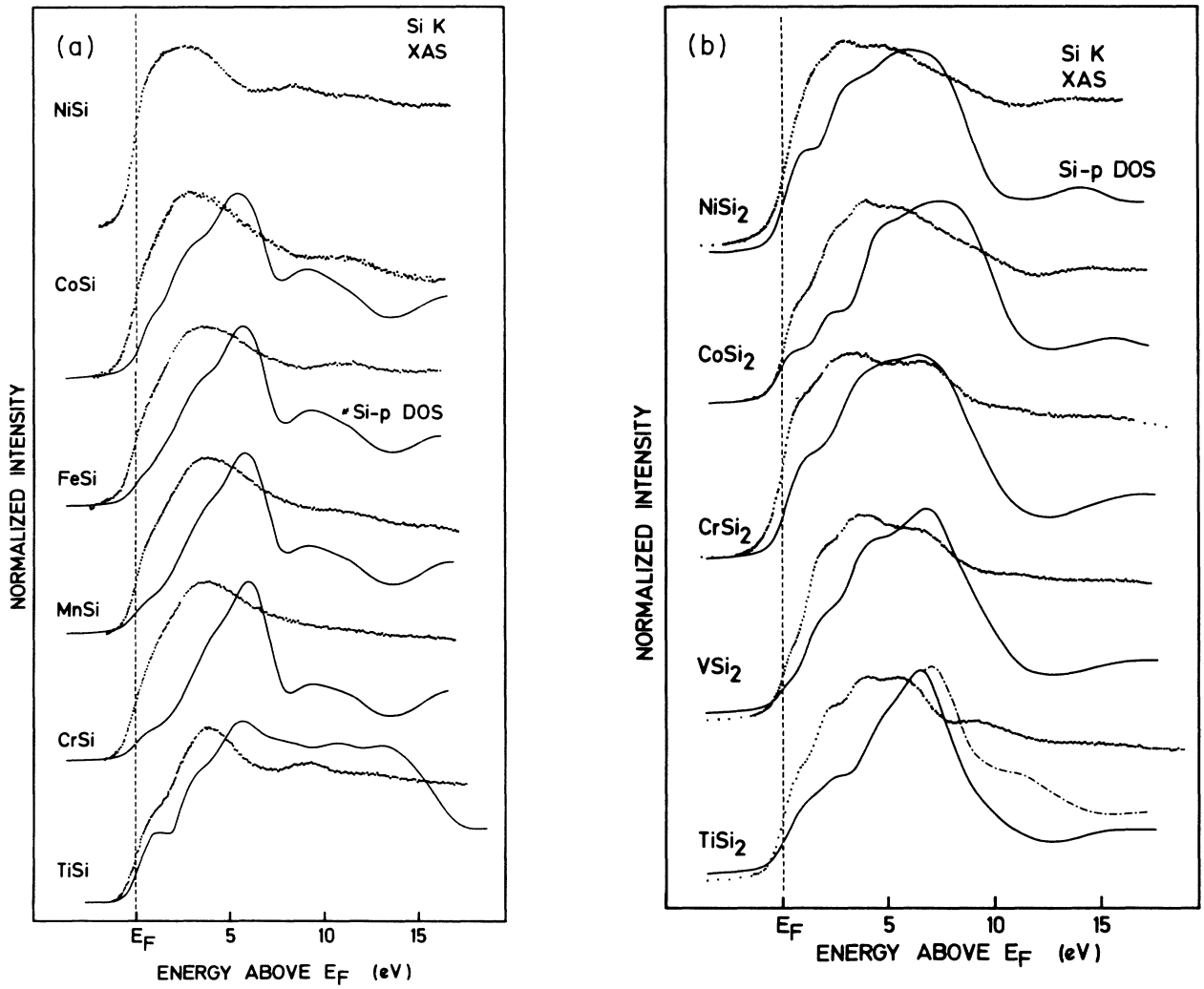

FIG. 1. Comparison of the measured Si K ($1s$) XAS spectra of (a) transition-metal silicides and (b) transition-metal disilicides with calculated partial density of states (Si p) curves. The partial DOS curves have been broadened as described in Sec. II B. Here, and throughout this paper, experimental data are given as dots and theoretical curves are lines.

lations with experiment for $TiSi_2$. Finally, after some comparison between theory and experiment for other silicides (Sec. III F), Sec. IV discusses how the core-hole effects in Si K XAS fit into the general pattern of core-hole effects.

II. METHODOLOGY: DETAILS OF EXPERIMENT AND CALCULATIONS

A. Experimental details

The polycrystalline samples of transition-metal silicides were prepared by indirect rf heating under clean Ar in a cold crucible, where necessary samples were vacuum annealed. X-ray diffraction was used to check that no sample was used unless the quantity of second phases was below 3%. The ingots of the silicides were cut into suitable pieces by spark erosion. They were then polished using Si-free abrasive and scraped *in situ* under ultrahigh vacuum with a ceramic file. We know from parallel x-ray photoelectron spectroscopic measurements that this procedure yields clean surfaces.[15–18]

The XAS spectra were measured in total photoelectron yield mode using radiation from the Daresbury and BESSY synchrotrons which was monochromated using a double-crystal monochromator fitted with InSb crystals.

The Auger spectra were measured at $\sim 10^{-10}$ Torr with a photoelectron spectrometer using Bremsstrahlung radiation to excite the Si 1s core holes. To avoid excessive absorption of Bremsstrahlung beyond the Al 1s edge, a Be window was used in place of the normal Al window to separate the x-ray anode from the sample chamber. X-ray emission results presented here are either from the published literature or were measured on a crystal spectrograph of the Johann type described elsewhere.[19]

B. Computations

In this paper our interest will be focused on description of localized excitations in the context of x-ray and other spectroscopies in which a core hole is present in the final state. The theoretical investigation presented consists of three complementary approaches. The first two belong to "heavy" first-principles electronic structure calculations, and the third is a semiempirical simulation of core-hole effects by the Clogston-Wolff model,[20,21] using the ground-state partial DOS as an input. The first-principles calculations have no variable parameters. The first group are "standard" band-structure calculations with varying degrees of approximation designed to save computer time. The second is a band-structure calculation with explicit inclusion of a core hole.

All first-principles calculations were carried out within the local-density framework with the Hedin-Lundqvist exchange-correlation potential and using a scalar-relativistic Hamiltonian (no spin-orbit coupling), which also treats all core electrons with a self-consistent procedure. In Table I we list the materials which were investigated, along with their structure and space-group symmetry, and, in the last column, the variety of computational methods which were applied. The most widely

TABLE I. Crystal structures for silicides and computation schemes used (see text for explanation of symbols).

Material	Type	Space-group symmetry	Reference	Computation
Ni_2Si	$PbCl_2$ ($C23$)	*Pnma*	a	*A*
Co_2Si	$PbCl_2$ ($C23$)	*Pnma*	a	*A*
TiSi	MnB ($B27$)	*Pnma*	b	*A,C,D*
CrSi	FeSi ($B20$)	$P2_13$	c	*A*
MnSi	FeSi ($B20$)	$P2_13$	c	*A*
FeSi	FeSi ($B20$)	$P2_13$	d	*A*
CoSi	FeSi ($B20$)	$P2_13$	c	*A,C*
NiSi	MnP ($B31$)	*Pnma*	e	*A,B*
$TiSi_2$	$TiSi_2$ ($C54$)	*Fddd*	f	*A,C,D*
VSi_2	$CrSi_2$ ($C40$)	$P6_222$	g	*A*
$CrSi_2$	$CrSi_2$ ($C40$)	$P6_222$	g	*A*
$Mn_{35}Si_{65}$	Mn_4Si_7	*P4c2*	a	
$FeSi_2$	$FeSi_2$	*P4/mmm*	h	
$CoSi_2$	CaF_2 ($C1$)	*Fm3m*	i	*A*
$NiSi_2$	CaF_2 ($C1$)	*Fm3m*	i	*A*

[a] *Pearson's Handbook of Crystallographic Data*, edited by P. Villars and L. D. Calvert (American Society of Metals, Metals Park, Ohio, 1985).
[b] *Structure Reports*, edited by J. Trotter (International Union of Crystallography, Bohn and Schelten at Holkena, Utrecht), Vol. 26, p. 18.
[c] *ibid.*, Vol. 3, p. 14.
[d] *ibid.*, Vol. 11, p. 146.
[e] *ibid.*, Vol. 35A, p. 86.
[f] *ibid.*, Vol. 7, pp. 12 and 95.
[g] *ibid.*, Vol. 8, p. 112.
[h] *ibid.*, Vol. 24, p. 78.
[i] *ibid.*, Vol. 13, p. 90.

used, indicated as type *A* in Table I, was the augmented-spherical-wave (ASW) method[22] with a minimal basis set. This set includes Si 3*s* and 3*p* on the Si site and 3*d*, 4*s*, and 4*p* on the 3*d* transition-metal (TM) sites. The internal summation was extended to $l=2$ for the Si and to $l=3$ for the metal. With this basis we describe all the occupied valence levels without using excessive computer time. The description of the unoccupied levels, especially at high energies, is less reliable using this basis set and for some test cases with 3*d* silicides we also included the Si 3*d* ASW's directly. We refer to these calculations as type *B* in Table I.

Next, for selected cases the localized–spherical-wave (LSW) method[23] was used with an extended set of functions[24] which includes Si 3*s*, 3*p*, 3*d*, 4*s*, 4*p*, and 4*f* and TM 3*d*, 4*s*, 4*p*, and 4*d* augmented SW's. These calculations are referred to as type *C* in Table I. The number of **k** points used in an irreducible part of the Brillouin zone (IBZ) was varied from 10 for high-symmetry cubic cases to 128 for hexagonal structures. Self-consistency was assumed to have been achieved when the partial charges in the atomic spheres varied less than 10^{-5} electron per iteration. Then the partial densities of states histograms were calculated with the number of **k** points in the IBZ varying from 165 to 1376 to maintain similar and satisfactory levels of sampling density for different BZ of different materials. Briefly, the results of comparisons of these methods were as follows.

(a) The minimal basis set calculations gave a reasonable description of the trends in (partial) DOS up to approximately 6 eV above E_F.

(b) Increasing the basis set gave shifts of a few hundred meV, even for the occupied states, so that the extended basis set is clearly desirable for detailed studies of self-energies. At 5 eV above E_F, shifts between different basis-set calculations were typically 0.5 eV.

(c) The largest basis-set calculation increased the density of states at, for instance, 10 eV above E_F, by about 30%.

The first class of calculations, described above, were all "standard" band structures, i.e., ground-state calculations. In order to investigate theoretically the influence of the core hole left behind in XAS, we performed a second class of (supercell) calculations where the excited atom (an atom with an inner-shell core hole) is formally treated as an impurity. Such an approach allows in a natural way for the symmetry breaking of the system and describes self-consistently the charge redistribution induced by the core hole. In this approach we also employed the LSW method. In the case of $TiSi_2$, the supercell contained 16 Si and 8 Ti atoms, i.e., it was four times bigger than the unit cell. The size of the supercell is important, and ultimately it should be large enough to inhibit interaction between excited atoms in neighboring supercells. Finally, local partial DOS obtained on a core ionized site was used to calculate the KL_1V Auger spectra as well as the *K* XAS spectrum.

The third class of calculations involved the Clogston-Wolff (CW) method. CW models have been used by several authors[11,21,25] to simulate spectra of impurities and core-hole effects. Our own version is a generalized CW model in which the strength of the hybridization between impurity and host may be varied in order to account for the contraction of the wave functions on the ionized site as a result of the core-hole potential. This version can reproduce almost exactly the density of states obtained by Korringa-Kohn-Rostoker (KKR)–Green's-function, imbedded-impurity calculations.[21] However, those studies showed that for *s* and *p* bands of the early, simple metals the strength of the hybridization was essentially unaffected by the core-hole potential. Therefore, in this work we keep the parameter which accounts for this hybridization unchanged from the host value, although a small reduction would probably be more physical. The only important parameter in the simulations is thus the energy shift, Δ, of the effective atomic level at the impurity site.[26]

While it is, in principle, feasible to make *ab initio* calculations for the Δ parameters in the CW calculations,[27,28] it would be a complex process and is not attempted here. In our opinion, a major advantage of the CW approach is that it allows us to study the local distortion of the DOS as a function of the strength of the core-hole potential by treating Δ as an adjustable parameter (different for different densities of states). As an input to the CW model we used the ground-state partial DOS from *ab initio* calculations described earlier in this section.

For all the calculations reported here the local partial DOS were convoluted with Lorentzian and Gaussian distributions in order to account for the core and final-state lifetimes and for instrumental effects, respectively. In Table II we show the values of broadening parameters used.[29–32]

III. RESULTS AND INTERPRETATION

A. Results of excited-state calculations and comparison with experiment

These calculations are an important reference point in our strategy because they represent an attempt to calculate the measured spectra without any free parameters. In Fig. 2 we compare the calculated local partial Si *s* and *p* DOS curves for ground-state $TiSi_2$ with those found for the final, excited state. In the latter the influence of the hole in the core state was self-consistently accounted for,

TABLE II. Broadening parameters used in convolution of local partial DOS. [All values in eV. Core-level lifetimes were selected from Ref. 29. The linear term, accounting for the lifetime of an electron or hole in the valence states, is a purely empirical value based on our experience in previous studies (Refs. 30–32).]

	Lorentzian FWHM (eV)	Gaussian FWHM (eV)
Si *K* XAS	$0.5+0.1(E-E_0)$	0.6
Si *K* XES	$0.5+0.1(E-E_0)$	0.6
Si $L_{2,3}$ XES	$0.1+0.1(E-E_0)$	0.3
Si KL_1V Auger	$1.65+0.1(E-E_0)$	0.6

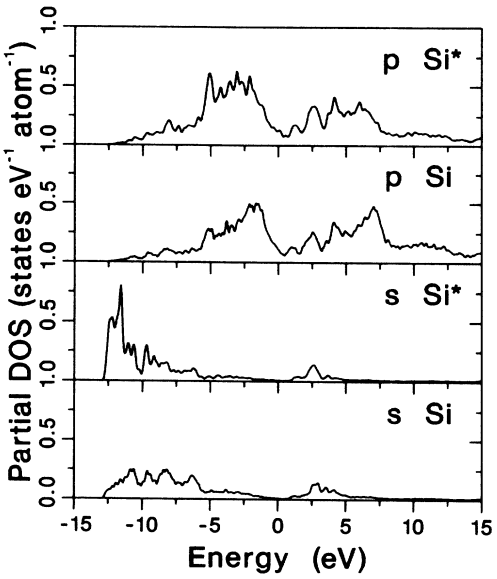

FIG. 2. Local, Si site projected, partial densities of states for $TiSi_2$ as calculated for the ground state and for the excited state with the presence of a core hole. The latter are indicated by an asterisk.

as described in Sec. II B.

First, we dismiss a trivial shift of the bottom of the s band by 160 meV. This arises because the simulation of the core hole introduces one hole per cell, instead of one per crystal. The shift is minor compared to the other effects we discuss.[33]

The most interesting effect we see in Fig. 2 is the shift of weight towards the bottom of the Si bands when a core hole is introduced. The curve shape for the local density of Si s states at a core ionized site is very different indeed from that of the unperturbed system, with a major peak near the bottom of the band. This effect is similar to that found in simulations of the core-hole effect on s states in pure light elements (Na, Mg, Al, Si) using various calculations.[10,34–37] Note also that the relative weight of Si s states above E_F is hardly influenced by the core hole. This can be understood if one remembers that a core-hole potential of a few eV is small by comparison with the large separation of the Si effective atomic s level from E_F.

The effect of the core hole on the partial density of Si p states is less dramatic in Fig. 2. We observe a shift in weight of the major peaks, in the range 3–11 eV below E_F, and also in the unoccupied states up to approximately 7 eV above E_F. It will be seen below that this change in shape will induce strong changes in spectral functions, even when lifetime and experimental broadening is taken into account. We also call attention to the increase in the area under the occupied Si s and p states curve below E_F. This corresponds to 0.88 and 0.21 extra electrons, respectively. It reflects the screening of the core hole. However, it is experimentally very difficult to detect changes in absolute intensity, and therefore absolute area, relating to this screening, so that it will not be extensively discussed here.

B. Si KLV Auger spectra

The x-ray-absorption results were presented in the Introduction. However, Si KLV Auger spectra are also important here because of the insight they give into the site- and symmetry-selected density of occupied states at a core ionized Si site.[9,23] It is accepted that the Auger transition matrix element is short ranged, so that only valence states with weight at the Si site contribute significantly to the spectrum. The density of states probed is that of a core ionized site because there is a core hole in both initial and final states. Furthermore, the angular parts of the Auger matrix elements are in the ratio $s:p = 3:1$ for KL_1V and 1:3 for $KL_{2,3}V$.[10,34,35] Thus the main features of s and p DOS may be recognized by comparing the KL_1V and $KL_{2,3}V$ spectra, although the radial parts of the matrix elements do modify the intensity ratios derived from the angular parts. In this paper we only discuss the Si KL_1V spectra, which show both a peak centered at 12–13 eV due to Si s states and at ~5 eV due to Si p states.[38]

We note that the one-electron binding energies of the

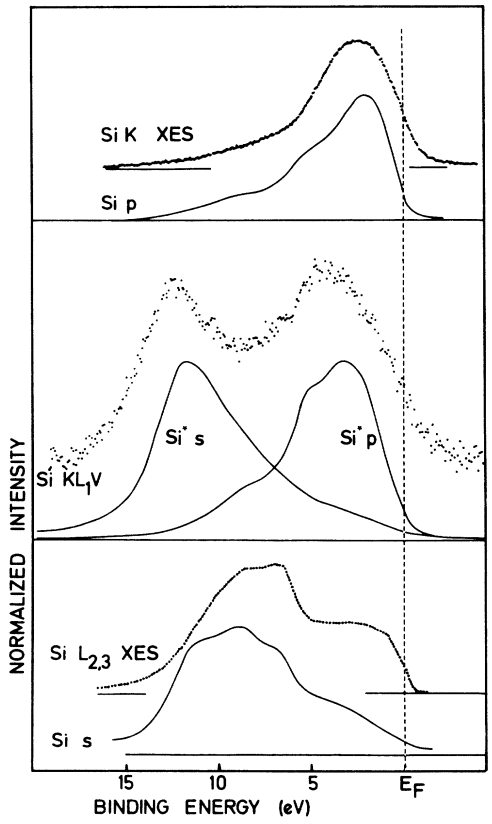

FIG. 3. Comparison of broadened partial DOS with AES and XES spectra for $TiSi_2$. The ground-state Si s DOS is compared to the Si $L_{2,3}$ emission spectrum in the lower panel, the ground-state Si p DOS is compared to the Si K emission spectrum in the upper panel. In the middle panel the Si s and p DOS for the excited state with the presence of a core hole, indicated by Si*, are compared with the Si KL_1V Auger spectrum. Si* s and Si* p are normalized to the same height. The broadening of the local DOS is described in Sec. II B.

Si s and p peaks given by Auger spectra are higher than those found in, for instance, x-ray-emission experiments (see Fig. 3 and Sec. III C). This is a known effect and is attributed primarily to the influence of the core-hole potential.[9,10,34–37]

C. Comparison of partial DOS and excited-state calculations core-hole effect with experiment

In Fig. 3 we compare local, partial Si DOS with various experiments. This picture will be used to illustrate that there are experimental shifts in peaks due to different, occupied partial DOS, according to whether or not a core hole is present in the final state. In addition, we will see that the calculated and experimental shifts are similar. Starting with data on the occupied s states, the Si s DOS curve (broadened as described in Sec. II B) in the lower panel of Fig. 3 is compared with the experimental Si $L_{2,3}$ x-ray-emission-spectroscopy (XES) curve[39] because there is no core hole in the final state in this process. Also dipole selection rules restrict valence-band hole effects in $L_{2,3}$ XES to Si s and d states and the d states play only a minor role near E_F (see, e.g., Ref. 1). The Si $L_{2,3}$ XES curve resembles the broadened Si s DOS curve quite closely, with the major intensity between 6.5 and 12 eV below E_F. The largest differences are relatively lower experimental intensity at the bottom of the band, possibly due to energy dependence of the matrix elements, and relatively higher experimental intensity close to E_F, where the Si d states become more important. The differences in peak positions are <1 eV and the degree of agreement indicates the relative unimportance (here) of energy-dependent exchange and correlation effects, which are not treated in the DOS calculation.[40] However, we will find that even the small differences observed are troublesome and sometimes detract from the degree of agreement between theory and experiment.

The Si K x-ray-emission spectrum, shown in the upper panel, probes the local density of Si p states and the agreement of its shape with the broadened ground-state Si p DOS (solid curve) is good. The major peak positions (experimental, ~ 2.4 eV; theory, ~ 2.1 eV) are similar; both curves show a long tail to high binding energies, and the major difference is a slightly broader experimental peak.

As stated in Sec. III B, the Si KL_1V Auger spectrum gives us data on the occupied Si states in the presence of a core hole. Thus the experimental peaks due to Si s and p states at ~ 13 eV and ~ 4–5 eV below E_F, respectively, lie much deeper than found in XES, as shown in the middle frame of Fig. 3.

In the middle frame of Fig. 3 we also compare the measured KL_1V Auger spectrum with the broadened Si s and Si p local partial DOS obtained in the presence of a $2s$ core hole (Si* s and Si* p, respectively). The calculated curves are normalized to the same height. Note that the theoretical curves lie much deeper than those in the absence of a core hole given in the top and bottom frames. The agreement with experiment is rather good, indicating that the calculations gives the correct peak positions and the correct shifts with respect to the ground-state DOS.

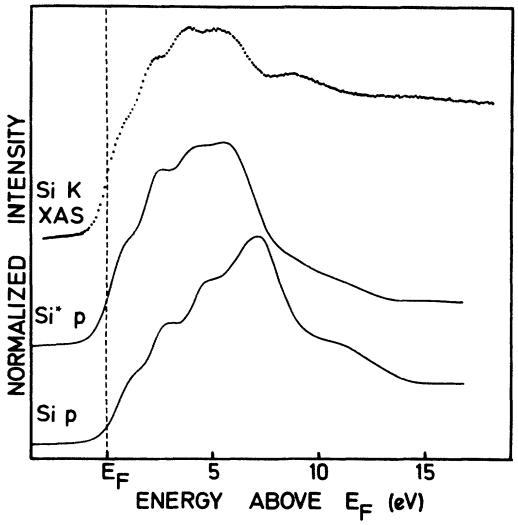

FIG. 4. Comparison of the Si K XAS of $TiSi_2$ with the computed local density of Si p states. Both the ground-state calculation, lower curve, and the calculation for a core ionized Si site, middle curve, are given as solid lines. The broadening of the local DOS is described in Sec. II B.

The main conclusion of the results in Figs. 2 and 3 described above is that the self-consistent calculation of final states with an ionized core gives an essentially proper description of the core-hole effects on the occupied states. We may thus expect similar quality of the description of the unoccupied states relevant to XAS. This is shown in Fig. 4. In the calculation the core hole is seen to shift weight to the peaks and shoulders nearer to the threshold. The result is in rather good agreement with the shape of the experimental spectra up to ~ 6 eV above E_F. This gives us confidence that the core-hole potential is indeed the major factor behind the differences between spectra and partial DOS curves in Fig. 1, at least for the first 6 eV above the threshold.

Note that the calculations yield far less weight in the region high above the threshold than is actually observed. We do not believe this is due to problems with background subtraction as the slope of the background below threshold is flat and monotonic in this region. There is always a problem of incomplete basis sets in the calculation, because the large lifetime broadening of high-energy unoccupied states (e.g., more than 15 eV above E_F) leads to their giving a spectral weight in the region 6–15 eV above E_F. However, the XAS spectra show no major peaks outside the range illustrated so that again this contribution is too weak to explain the discrepancy. The last possibilities we can list are the energy dependence of the single-particle XAS matrix elements and many-body excitations. The first of these two is easier to test and we hope to write the computer codes necessary for this test in the foreseeable future.

D. Simulations of the core-hole effects with a generalized Clogston-Wolff model

As stated in Sec. II B, one of the major advantages of models like the Clogston-Wolff model is that it allows one

As stated in Sec. II B, one of the major advantages of models like the Clogston-Wolff model is that it allows one to compute in a simple way the effect of a core-hole potential as it is slowly increased. We thus indicate some of the general trends, using the CW model, before attempting to reproduce measured spectra. We start in Fig. 5 with the Si s DOS for which the band edge is 13.6 eV below E_F. Figure 5 illustrates that even a small attractive potential causes a strong shift of weight to the high binding-energy edge of the band. This shift becomes stronger as Δ is increased and eventually the potential is strong enough to split off a bound state at the bottom of the band, as seen in the $\Delta=-5$ and $\Delta=-10$ eV curves. This bound state has the majority of the Si s weight, as can be seen from the dramatic decrease in the state density in the band region. In this example the core-hole potential has a strong effect on the *shape* of the occupied state distribution, but above E_F it only influences the weight; there is hardly any influence on the shape. This is by no means always the case.

In order to judge the influence of the attractive potential on the spectra, it is sensible to broaden the spectra to simulate core-hole lifetime and instrumental broadening, as well as the valence state lifetime broadening. Also, we normalize the spectra to a constant height, just as we would do with experimental spectra. The results are shown in Fig. 6(a) for the occupied Si s DOS, in Fig. 6(b) for the occupied Si p DOS, and in Fig. 6(c) for the unoc-

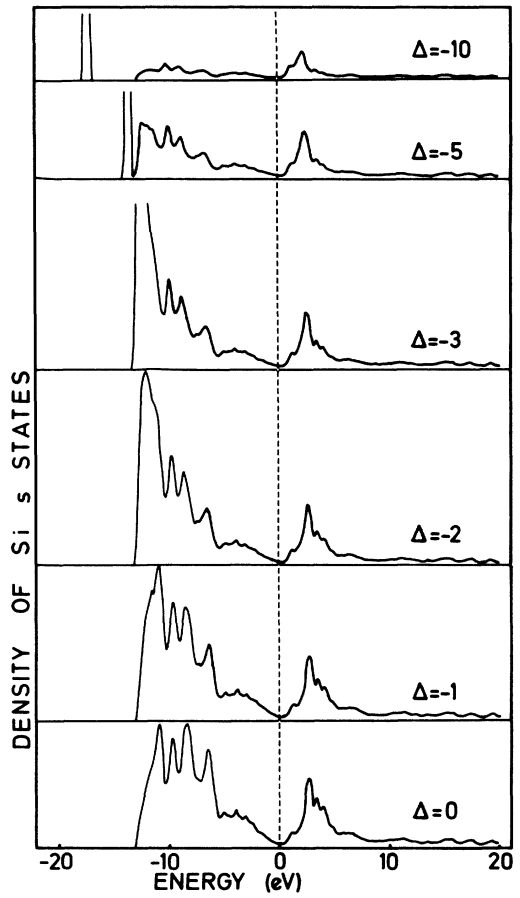

FIG. 5. The influence of an increasing Si core-hole potential on the local density of Si s states. The DOS as calculated for Fig. 2, without a core hole, has been broadened by a 0.3-eV Gaussian to smooth out details of the structure not relevant here. Δ refers to the attactive potential parameter used in the CW model (in eV). The curves have been normalized to keep their area constant although that requires a truncation of the peak growing at the bottom of the valence states for $\Delta \geq 3$ eV.

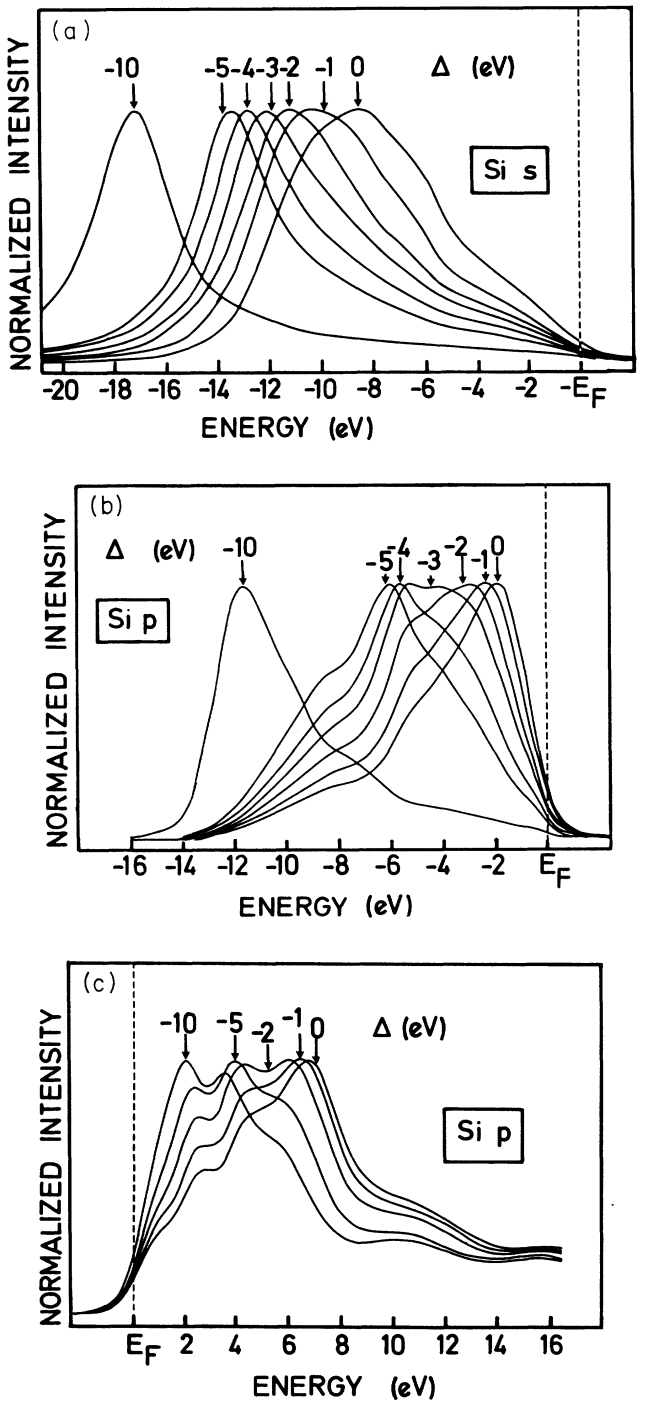

FIG. 6. Clogston-Wolff simulations of the distortion of the local partial density of Si states at a core ionized site using the ground-state DOS of $TiSi_2$. (a) Occupied s states; (b) occupied p states, and (c) unoccupied p states. The theoretical curve broadening is as described in Sec. II B.

cupied Si p DOS. The occupied Si s DOS is clearly very sensitive to the attractive potential and the peak moves rapidly to higher binding energies (BE). This is consistent with the shift observed in the high BE peak of the Si KL_1V Auger spectrum which was attributed to the local density of Si s states. The "best" description in the CW model of the observed KL_1V AES peak was obtained with $\Delta=-3.2$ eV as will be described in Sec. III E. We do not have experimental XAS data relating to the unoccupied DOS for Si s states, and thus we do not present CW curves for these states.

In Fig. 6(b) we consider the effect of the attractive potential on the occupied Si p states. Here we see that the unperturbed Si p DOS has low weight near E_F, and a peak at ~ 2 eV, in agreement with the Si K ($1s$) x-ray-emission data (upper frame of Fig. 3). Again an attractive potential at the Si site is seen to shift weight to higher BE. However, here a Δ of even -10 eV does not produce a split-off bound state, primarily because it is a wide band and the effective Si p atomic level of the unperturbed system is very far above the bottom of the band. Note that the curves produced for Si p states in $TiSi_2$ by the CW model with $\Delta\sim -3$ eV are rather complex, having a broad, double-peaked structure.

From the above discussion it is clear that an attractive potential in the CW model can distort the local density of Si s and p states in such a way as to reproduce the KLV Auger spectral features (see also Ref. 11). Thus it is reasonable to apply the CW model to XAS, and in Fig. 6(c) we consider the distortion of the unoccupied Si p DOS. The unperturbed p DOS curve has a major peak at approximately 6.5 eV and several small steps leading down to a low weight near E_F. Application of an attractive potential causes transfer of weight below E_F, but this is not visible in Fig. 6(c) because the spectra are normalized to the same height. The distortion of the shape is, however, very clear and substantial for small values of Δ (up to ~ -3 eV) although the changes become more gradual as Δ is still further increased.

E. Comparison of generalized CW calculations with experiment for $TiSi_2$

We now consider the capability of the CW model to simulate actual spectra from ground-state spectra. We know from previous work that the CW calculations give a very good simulation of local-density-approximation (LDA)–KKR–Green's-function calculations in which a core hole is simulated by embedding a "$Z+1$" atom in a periodic matrix.[21] However, those LDA-KKR calculations do not always describe XAS spectra well.[41]

In this work the CW model was used with free Δ parameters to simulate experimental spectra. One may ask in how far the agreement achieved (which is very good, as shown in Figs. 7 and 8) is artificial. For instance, the influence of energy dependence of exchange and correlation, or dynamical effects could be lumped together with core-hole effects.[42] The answer to this question will be case dependent. Here, however, we have also the results of *ab initio* calculations which are free of adjustable parameters. These *ab initio* calculations did not treat either self-energy or dynamical effects. Therefore, on the basis of the general agreement of all three results (experiments, CW modeling, and *ab initio* calculations) we can exclude a major role of self-energy and dynamical effects for $TiSi_2$ in the energy range considered here.

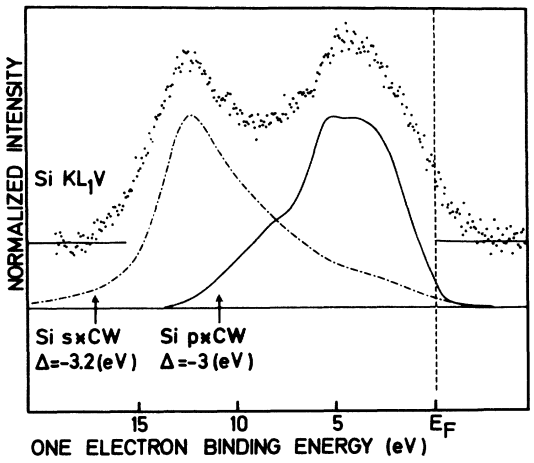

FIG. 7. Simulations of the local density of Si s and p states at a core ionized site using the ground-state DOS of $TiSi_2$ and an attractive core-hole potential in the generalized Clogston-Wolff model. The CW curves are compared with the experimental KL_1V Auger spectrum. The theoretical curve broadening is as for the AES curve in Fig. 3.

We now consider the CW simulations of actual spectra, starting with the $TiSi_2$ Auger data (Fig. 7). The application of the CW model with $\Delta=-3.2$ eV to the partial density of s states in $TiSi_2$ leads to a strong peak at the bottom of the band, which on broadening closely resembles the high BE peak of the Si KL_1V Auger spectrum. A larger value of Δ would rapidly lead to less agreement because it would result in bound-state formation, with most of the predicted spectral weight in a narrow peak

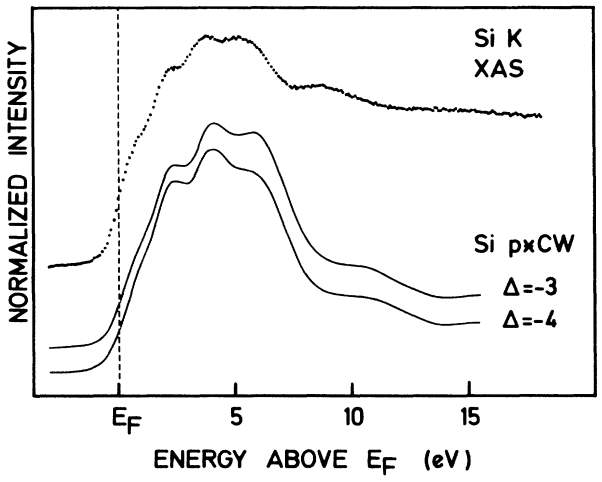

FIG. 8. Comparison of Si K XAS curves and simulations based on the density of unoccupied Si p states and the generalized CW model with $\Delta=-3$ and -4 eV for $TiSi_2$.

below the bottom of the band [see, e.g., Fig. 6(a)]. Here, however, the CW model clearly leads to a good simulation of the available data.

The application of the CW model with $\Delta=-3.0$ eV shifts the peak of the occupied $TiSi_2$ Si p partial DOS to $\sim 4-5$ eV below E_F, which is in good agreement with the position of the peak attributed to Si p states in the KL_1V Auger spectrum. The choice of the "best" value of the occupied Si p state Δ is relatively unambiguous because the peak shifts rapidly as Δ is increased [see Fig. 6(b)]. The same is not true for the CW simulations of the Si K XAS spectra, which change rather slowly as Δ is increased [see Fig. 6(c)]. As shown in Fig. 8, the CW model with $\Delta=-4$ eV gives a reasonable simulation of the spectra, up to ~ -6 eV above threshold, although the $\Delta=-3$-eV curve is not noticeably worse. The uncertainty in the precise value of Δ is increased by the failure of all our calculations to reproduce the large intensity more than 6 eV above E_F.

In summary of the results presented in Fig. 7 and 8, we may state that the agreement between the Auger spectra and the CW simulations with input of the ground-state DOS is excellent, as is also the case for the K XAS spectra up to 6 eV above E_F. The CW results are even better than the simulations from *ab initio* calculations, especially for the p peak. However, more work is necessary before too much physical significance can be attached to the numerical values of Δ.

F. Comparison of simulations with spectra of other silicides

Although detailed comparison of the simulations with spectra for each and every silicide is superfluous, we prefer not to base our conclusions on results from just one compound. We chose TiSi to test the influence of stoichiometry and $NiSi_2$ to test the influence of changing the transition metal on the quality of our simulations and the conclusions concerning the importance of core-hole effects.

Figure 9 illustrates various approaches to simulation of the Si K XAS spectrum of TiSi. The Si p DOS has, of course, the main peaks at too high energies. Introduction of a core hole at a Si site in the supercell calculation results in a shift of weight to the lower-energy peaks and the overall shape of the local Si p DOS curve at the ionized Si site resembles quite closely the XAS spectrum up to ~ 6 eV above E_F. Note, however, that the calculation produces too much structure in the region 3–5 eV above E_F. There is again too little weight at energies higher than 6 eV above E_F in the calculated curve, and again we believe that the first approach to this problem should be computation of the single-particle matrix elements.

The best curves from CW treatment of the partial DOS curve were those with $\Delta=-4$ eV. The -4-eV curve, shown in Fig. 9, has its main weight around ~ 4 eV above threshold, as in the experiment, but shows a double-peaked structure not observed in experiment. Increased lifetime broadening would not greatly improve agreement with experiment. Thus we believe that self-energy effects are the most likely reason for failure to simulate the spectra more accurately. However, it should be stressed that the CW treatment of the unoccupied DOS does do one thing correctly: it shifts weight to the lower-energy features and improves agreement with experiment in the region 0–6 eV above threshold.

Also for $NiSi_2$ (Fig. 10), the CW treatment improves

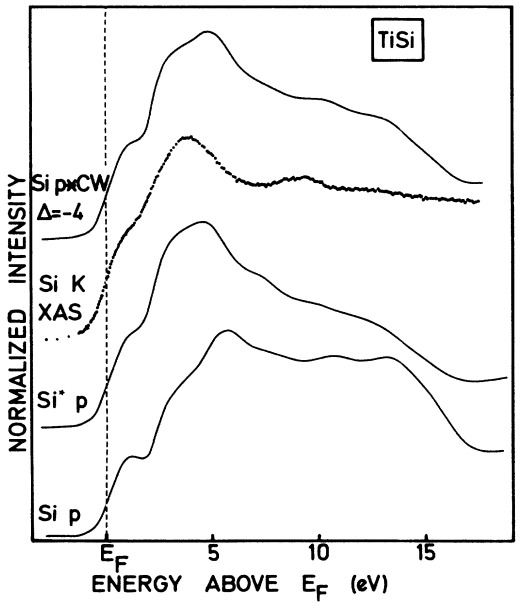

FIG. 9. Comparison of the experimental Si K XAS spectrum of TiSi (dots) with the partial density of Si p states, the partial density of Si p states calculated in the presence of a core hole (Si* p), and the partial density of unoccupied Si p states treated by the Clogston-Wolff model with Δ set at -4 eV.

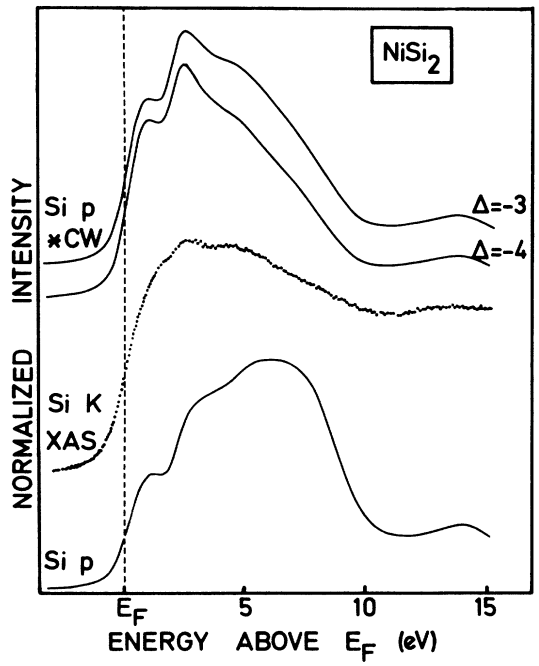

FIG. 10. Comparison of the experimental Si K XAS spectrum of $NiSi_2$ (dots) with the partial density of Si p states, and the partial density of unoccupied Si p states treated by the Clogston-Wolff model with Δ set at -3 and -4 eV.

TABLE III. "Best" values for the core-hole potential, Δ, from simulation of experimental spectra from unperturbed DOS curves (all values in eV).

Material	Δ*s* (occ) from KL_1V	Δ*p* (occ) from KL_1V	Δ*p* (unocc) from XAS
$TiSi_2$	3.2	3.0	3–4
TiSi			3–4
$NiSi_2$			3–4

agreement with experimental XAS data close to E_F. We again see the missing weight more than ~7 eV above E_F, and note that in this case the effect is aggravated because we have used a partial DOS curve from a calculation without an extended basis set. Also the Si *K* edge is broader than in other compounds for some reason. However, the CW treatment shifts weight towards threshold so that the maximum is at ~2.5 eV (experiment ~2.6 eV) instead of at ~6 eV as in the partial Si *p* DOS of the unperturbed lattice. The calculated CW curves also have a shoulder at 1.0 eV. Its position is strongly dependent on the broadening and it may be associated with the experimental shoulder near 1.5 eV. A further shoulder near 4.5 eV in the experimental curve may be associated with a similar feature at the same energy. Thus, in summary, treatment of the unperturbed partial density of Si *p* states with the CW model treatment gives reasonable agreement with Si *K* XAS of $NiSi_2$ up to ~7 eV above E_F, and the major disagreements are in the intensity at higher energies and the widths of the features.

IV. SUMMARY AND CONCLUSIONS

In this paper we have presented evidence of significant differences between ground-state site- and symmetry-selected DOS and experimental Si *K* XAS data for transition-metal silicides (Sec. I). For a test case we have also taken into consideration experimental data on Si *KLV* Auger spectra, which are known to give site-specific information on the local DOS in the presence of a core hole (Sec. III B). We find that by introducing the core hole at the Si site and carrying out self-consistent calculations within a supercell approach, we can properly describe the changes of spectral distributions of valence and unoccupied states induced by that hole. These changes improve the description of *KLV* Auger spectra, as well as the description of Si *K* x-ray-absorption spectra. In particular for the latter case, the shift of intensity towards the threshold enables us to conclude that the initial discrepancies (Fig. 1) were indeed primarily caused by core-hole effects.

We have then used an extended Clogston-Wolff model to investigate the development of core-hole effects and found that it can give a good description of core-hole effects with reasonable values for the core-hole potential parameters, Δ. The values found are summarized in Table III and give a general idea of their size for the Si *K* level. Δ values of 3.2 eV for Si *s* states and 3–4 eV for Si *p* states gave reasonable agreement between theory and experiment for all cases tested, although one should be cautious about attaching too much significance to the precise numerical values at this stage. It is at least clear that Δ is much smaller than the naked Coulomb interaction between core and valence wave functions, as a result of screening effects. On the other hand, values of typically 3 eV are not so much smaller than the potential at the bottom of the band that they can be neglected entirely. A very practical use of the CW model is to test whether or not differences between XAS spectra and ground-state DOS *can* be attributed to core-hole effects. If the values of the Δ parameters turn out to be transferable, other uses can be envisaged, but more applications to other

TABLE IV. Approximate core-hole potentials (Δ) and valence-band widths (*W*) relevant to XAS spectra, along with a summary of their behavior.

Level	Materials	Δ (eV)	*W* (eV)	Multiplet interaction	Behavior
Si *K*	silicides	3–4	5–10	weak	Core-hole effect is the most important after solid-state band structure. Effects are not negligible.
$L_{2,3}$	early 3*d* transition metals	2–4	5–8	~5 eV	Core-hole and band-structure effects must be treated on the same footing. Multiplet effects are not negligible.[a]
$L_{2,3}$	3*d* transition-metal compounds	2–6	2–6	~5 eV	Atomiclike spectra often observed. Core-hole and multiplet effects dominate.[b]
$M_{4,5}$	lanthanides and their compounds	~10	<0.2	~5 eV	Atomiclike multiplet structure always dominates but crystal fields, etc., may influence terms observed.[c]

[a]References 2 and 3.
[b]Reference 43.
[c]Reference 44.

types of materials are desirable. Thus our main conclusions are as follows.

(1) The measured Si K XAS spectra from transition-metal silicides cannot be successfully obtained from partial Si p DOS of the ground state, as concluded earlier for Al K XAS.[40]

(2) The differences between (broadened) DOS curves and measured spectra up to ~ 6 eV above threshold are primarily due to the core-hole potential.

(3) The core-hole effects can be successfully described by *ab initio* calculations which explicitly include the presence of the hole in the excited state.

(4) The core-hole effect can be successfully simulated by a Clogston-Wolff model.

We found three problems in this work.

(1) We have no quantitative explanation of why the theoretical curves show much less weight at high energy than the experimental data. We suspect this is due to single-particle matrix elements.

(2) We have been forced to use empirical values for the imaginary part of the self-energy (lifetime broadening) of both the valence and the unoccupied states. This is unsatisfactory.

(3) We are continually confronted with small differences in peak positions found theoretically and experimentally. These are attributed to many-body interactions (i.e., self-energy effects). Of course, points (2) and (3) are not entirely separable.

To place these studies of Si K XAS spectra in context, we compare their behavior with that for the $L_{2,3}$ edges of $3d$ transition metals and the $M_{4,5}$ edges of rare earths. As a first ansatz one would imagine that large core-hole potentials (Δ) and small valence-band widths (W) would favor strong distortion of the spectra with respect to the band-structure limit. These data are summarized in Table IV. The data do indeed support the ansatz, but we note that in intermediate cases ($L_{2,3}$ XAS) the type of spectrum observed depends strongly on the chemical environment.

While there has been much consideration of core-hole effects for other core levels, few have been studied in the same detail as those listed in Table IV. We may note, for instance, that the Δ and W parameters relevant to the much-studied $L_{2,3}$ edges of $4d$ and $5d$ transition metals (or K edges of $3d$ transition metals) are expected to be similar to those of the Si K levels in silicides. It is not clear to us if core-hole effects are actually weaker in those levels, or just harder to detect as a result of greater core-hole lifetime broadening. Detailed studies in this area are much needed.

---

*Present address: Zentral Institut für Chemische Analyse der Kernforschungsanlage Jülich, D-5170 Jülich 1, Federal Republic of Germany.

†Present address: Natuurkundig Laboratorium, Vrije Universiteit, Postbus 7161, NL-1007 MC Amsterdam, The Netherlands.

‡Present address: Daresbury Synchrotron Laboratory, Daresbury, Warrington WA4 4AD, United Kingdom.

[1]D. J. Fabian, L. M. Watson, and C. A. W. Marshall, Rep. Prog. Mod. Phys. **34**, 601 (1972); G. Wiech, in *Emission and Scattering Techniques, NATO Advanced Study Institute Series B: Physics,* edited by P. Day (Reidel, Dordrecht, 1981), p. 103.

[2]J. Fink, Th. Müller-Heinzerling, B. Scheerer, W. Speier, F. U. Hillebrecht, J. C. Fuggle, J. Zaanen and G. A. Sawatzky, Phys. Rev. B **32**, 4899 (1985).

[3]J. Zaanen, G. A. Sawatzky, J. Fink, W. Speier, and J. C. Fuggle, Phys. Rev. B **32**, 4905 (1985).

[4]Classic papers in this area include G. D. Mahan, Phys. Rev. **163**, 612 (1967); P. Nozières and C. T. De Dominicis, *ibid.* **178**, 1097 (1969); L. Hedin, in *X-ray Spectroscopy,* edited by L. V. Azaroff (McGraw-Hill, New York, 1974), pp. 226ff.

[5]A. Kotani and Y. Toyozawa, J. Phys. Jpn. **35**, 1073 (1973); **35**, 1082 (1973); **37**, 912 (1974).

[6]K. Ohtaka and Y. Tanabe, Phys. Rev. B **28**, 6833 (1983); Y. Tanabe and K. Ohtaka, *ibid.* **29**, 1653 (1984); K. Ohtaka and Y. Tanabe, *ibid.* **30**, 4235 (1984), and references therein.

[7]C. O. Almbladh and L. Hedin, in *Handbook of Synchrotron Radiation, Vol. I,* edited by E. E. Koch (North-Holland, Amsterdam, 1983), p. 607 and references therein.

[8]L. G. Parratt, Rev. Mod. Phys. **31**, 616 (1959).

[9]R. Lässer and J. C. Fuggle, Phys. Rev. B **22**, 2637 (1980). Note that the ratio of the angular parts of the Auger matrix elements for s and p contributions to the KL_1V spectra was incorrect in this paper.

[10]J. C. Fuggle, in *Electron Spectroscopy,* edited by C. R. Brundle and A. D. Baker (Wiley, New York, 1981), Vol. 4, pp. 85ff and references therein.

[11]D. E. Ramaker, F. L. Hutson, N. H. Turner, and W. N. Mei, Phys. Rev. B **33**, 2574 (1986).

[12]J. C. Fuggle, Phys. Scr. T **17**, 64 (1987); P. J. W. Weijs, G. Weich, W. Zahorowsky, W. Speier, J. B. Goedkoop, M. Czyżyk, J. F. van Acker, E. Van Leuken, R. A. de Groot, G. van der Laan, D. D. Sarma, L. Kumar, K. H. J. Buschow, and J. C. Fuggle, *ibid.* (to be published).

[13]A. Bianconi, R. Del Sole, A. Selloni, P. Chiaradia, M. Fanfoni, and I. Davoli, Solid State Commun. **64**, 1313 (1987).

[14]X. Weng, P. Rez, and O. F. Sankey, Phys. Rev. B **40**, 5694 (1989).

[15]W. Speier, E. van Leuken, J. C. Fuggle, D. D. Sarma, L. Kumar, B. Dauth, and K. H. J. Buschow, Phys. Rev. B **39**, 6008 (1989).

[16]D. D. Sarma, W. Speier, R. Zeller, E. van Leuken, R. A. de Groot, and J. C. Fuggle, J. Phys. Condens. Matter **1**, 9131 (1989).

[17]W. Speier, L. Kumar, D. D. Sarma, R. A. de Groot, and J. C. Fuggle, J. Phys. Condens. Matter **1**, 9117 (1989).

[18]P. J. W. Weijs, M. T. Czyżyk, J. C. Fuggle, W. Speier, D. D. Sarma, and K. H. J. Buschow, Z. Phys. B **78**, 423 (1990).

[19]W. Zahorowski, J. Mitternacht, and G. Wiech (unpublished).

[20]P. A. Wolff, Phys. Rev. **124**, 1030 (1961); A. M. Clogston, *ibid.* **125**, 439 (1962); A. M. Clogston, B. T. Matthias, M. Peter, H. J. Williams, E. Corenzwit, and R. J. Sherwood, *ibid.* **125**, 541 (1962).

[21]W. Speier, J. F. van Acker, and R. Zeller, Phys. Rev. B **41**, 2753 (1990); J. F. van Acker, W. Speier, and R. Zeller (unpublished).

[22]A. R. Williams, J. Kübler, and C. D. Gelatt, Jr., Phys. Rev. B

19, 6094 (1979).

[23]H. van Leuken, A. Lodder, M. T. Czyżyk, E. Springelkamp, and R. A. de Groot, Phys. Rev. B **41**, 5613 (1990).

[24]M. T. Czyżyk, R. A. de Groot, G. Dalba, P. Fornasini, A. Kisiel, F. Rocca, and E. Burattini, Phys. Rev. B **39**, 9831 (1989).

[25]D. van der Marel, C. Westra, and G. A. Sawatzky, Phys. Rev. B **31**, 1936 (1985); D. van der Marel, J. A. Julianus, and G. A. Sawatzky, *ibid.* **32**, 6331 (1985).

[26]Apart from the approximations inherent in the application of our model approach to pure metals in a cubic environment, and discussed in Ref. 21, a further approximation is introduced by the application of this scheme to compounds. In general, symmetry lowering at the impurity site will result. The approximation here lies in the fact that we apply the CW model computation to the *s* or *p* projected partial DOS, and do not consider possible admixture of states of other, notably *d*, orbital symmetry. That these additional effects are not large in the case of core ionized Si in the transition-metal silicides follows from the general agreement we find with the results of the supercell calculations.

[27]See, e.g., A. K. McMahan and R. M. Martin, in *Narrow Band Phenomena,* edited by J. C. Fuggle, G. A. Sawatzky, and J. W. Allen (Plenum, New York, 1988), p. 133.

[28]O. Gunnarsson, O. K. Andersen, O. Jepsen, and J. Zaanen, in *Core Level Spectroscopy of Condensed Systems,* edited by J. Kanamori and A. Kotani (Springer, Heidelberg, 1988), p. 82; Phys. Rev. B **39**, 1708 (1989).

[29]K. D. Sevier, *Low Energy Spectroscopy* (Wiley-Interscience, New York, 1972), p. 230; M. O. Krause and J. H. Oliver, J. Phys. Chem. Ref. Data **8**, 329 (1979).

[30]J. E. Mueller, O. Jepsen, and J. W. Wilkins, Solid State Commun. **42**, 365 (1982).

[31]D. van der Marel, G. A. Sawatzky, R. Zeller, F. U. Hillebrecht, and J. C. Fuggle, Solid State Commun. **50**, 47 (1984).

[32]W. Speier, R. Zeller, and J. C. Fuggle, Phys. Rev. B **32**, 3597 (1985).

[33]We have made some test calculations for the core excited states with larger unit cells. There were small, but numerically significant differences for different core holes (e.g., 2*s* and 2*p*). We hope to investigate this further, but note that the diffrences were insufficient to influence any of the conclusions presented here.

[34]U. von Barth and G. Grossmann, Phys. Rev. B **25**, 5150 (1982).

[35]L. Hedin, J. Phys. (Paris) Colloq. **39**, C4-103 (1978).

[36]C. O. Almbladh and U. von Barth, Phys. Rev. B **13**, 3307 (1978).

[37]G. W. Bryant and G. D. Mahan, Phys. Rev. B **17**, 1744 (1978).

[38]We observed differences in the position of the peaks due to the *p* states in KL_1V and $KL_{2,3}V$ Auger spectra. The peaks were in general at ~ 0.5 eV higher BE in the $KL_{2,3}V$ spectra, but in the case of $TiSi_2$ the differences were as much as ~ 1.3 eV. We do not know the origin of this effect but suspect a role of multiplet interactions between the $2p$ hole and the unpaired valence electrons. As this paper is primarily concerned with core-hole effects in XAS, we do not discuss the discrepancies further here, but do note that a larger core-hole potential would have to be included to account for some of the $KL_{2,3}V$ spectra.

[39]G. Wiech (Si *K* of $TiSi_2$; new data) and E. Zöpf (Si $L_{2,3}$ of $TiSi_2$); Ph.D. thesis, University of Munich, 1973 (unpublished).

[40]Note that this is in contrast to our previous experience with NiAl; S. W. Kortboyer, M. Grioni, W. Speier, R. Zeller, L. M. Watson, M. T. Gibson, F. Schäfers, and J. C. Fuggle, J. Phys. Condens. Matter **1**, 5981 (1989).

[41]R. Zeller, Z. Phys. B **72**, 79 (1988).

[42]Strictly speaking, the self-energy for Auger and XAS experiments includes the core-hole potential. However, we separate the core-hole effect from the electron-electron interaction, which dominates the self-energy effects in photoemission and XES.

[43]See, e.g., T. Yamaguchi, S. Shibuya, S. Suga, and S. Shin, J. Phys. C **15**, 2641 (1982); G. van der Laan and B. T. Thole, Phys. Rev. Lett. **60**, 1977 (1988); F. M. F. de Groot, J. C. Fuggle, B. T. Thole, and G. A. Sawatzky, Phys. Rev. B **41**, 928 (1990).

[44]The atomic nature of the $M_{4,5}$ absorption edges of the rare earths was recognized in the 1930s [see the references cited in B. T. Thole, G. van der Laan, J. C. Fuggle, G. A. Sawatzky, R. C. Karnatak, and J.-M. Esteva, Phys. Rev. B **32**, 5107 (1985)]. X-ray dichroism due to magnetic and crystal-field effects is discussed in G. van der Laan, B. T. Thole, G. A. Sawatzky, J. B. Goedkoop, J. C. Fuggle, J.-M. Esteva, R. Karnatak, J. P. Remeika, and H. A. Dabkowska, Phys. Rev. B **34**, 6529 (1986) and J. B. Goedkoop, Ph.D. thesis, University of Nijmegen, 1989 (unpublished).